Aust. Met. Mag. 37 (1989) 141-153

Tropical forecasting: predictability perspective*

J. Shukla
Center for Ocean-Land-Atmosphere Interactions, Department of Meteorology, University of Maryland, USA

(Manuscript received October 1988; revised April 1989)

We present results of classical predictability studies and forecast experiments with observed initial conditions to show the nature of initial error growth and final error equilibration for the tropics and mid-latitudes separately. It is found that the theoretical upper limit of predictability of tropical circulation is far less than that of the mid-latitudes.

We have compared the error growth for a complete general circulation model to that for a dry version for the same model in which there is no prognostic equation for moisture, and diabatic heat sources are prescribed. It is found that the rate of growth of synoptic-scale errors for the dry model is significantly smaller than that for the moist model suggesting that interactions between dynamics and moist processes are one of the important causes of the degradation of predictability of atmospheric flows. In particular, we find that condensation processes are far more important than radiation processes. We have also shown that an improved treatment of the role of vegetation reduces systematic errors in forecasts over tropical land masses.

Finally, we present results of numerical experiments which have shown that correct specification of the slowly varying boundary condition of sea surface temperature produces significant improvement in the prediction of time averaged circulation and rainfall over the tropics.

Introduction

One of several empirical approaches to study the predictability of the atmosphere with respect to a particular model is to integrate the model starting from a given initial condition and repeat the integrations with slightly perturbed initial conditions, and to examine the rate at which the small initial error grows with time. The limit of predictability is then determined by the rate of error growth and the saturation value of the error. The growth rate is determined by the nature of nonlinear interactions and dominant instabilities, and the saturation value of the error is determined by the mechanisms responsible for equilibration of the amplitudes of the most energetic disturbances. In other words, the standard deviation of the day-to-day fluctuations is a direct measure of the saturation value of the error. Since the upper limit of predictability is generally defined as the time it takes for the initial error to grow to become comparable to the error between two randomly chosen maps, the quantitative value of the upper limit of predictability is a strong function of the magnitude of the day-to-day fluctuations.

A direct consequence of the above arguments is that even if the growth rates of the initial error were identical for the tropics and the mid-latitudes, the upper limit of determin-

* Based on an invited paper presented at the International Conference on Tropical Meteorology, Brisbane, July 1988.

istic predictability for atmospheric variables like temperature, pressure and wind would be far less for the tropics than that for the mid-latitudes. This is mainly because the magnitude of the day-to-day fluctuations of these variables for the tropics is far less than that for the mid-latitudes. Since tropical and extratropical flows interact strongly, whether the predictability of the tropical and extratropical flows can be examined separately will depend upon the relative magnitudes of the time-scale of interactions and the time-scale of saturation of initial error. Numerical experiments with large atmospheric models show (Shukla 1981, 1985) that it takes only 3-5 days for the initial tropical error to reach its maximum (saturation) possible value and therefore it is justifiable to examine the predictability of the tropical atmosphere separately.

The above conclusion of lower predictability for the instantaneous flow patterns in the tropics compared to that in the mid-latitudes was based on the assumption that the growth rate, as well as the initial error, is similar both for the tropics and the mid-latitudes. In reality, the initial errors are relatively larger for the tropics compared to the mid-latitudes and the growth rates of initial error can also be larger because of a stronger nonlinear feedback between dynamics and moist convection. In summary, the theoretical upper limit of predictability for tropical circulation variables would always be less than that for the mid-latitudes. The actual quantitative value of this theoretical upper limit will, of course, depend upon the particular model and particular circulation variable; however, for current global general circulation models for which the theoretical upper limit of predictability for the mid-latitude circulation is about 10-15 days, it is only about 3-7 days for the tropics.

In contrast, the prospects for predictability of space-time averaged tropical circulation are far better than those for the mid-latitude circulation (Charney and Shukla 1977; Shukla 1981). This is primarily because the day-to-day fluctuations are small in the tropics and the interannual variability of the time averages is largely determined by the changes in the slowly varying boundary conditions at the earth's surface. Therefore, for the time-scales at which anomalies in surface forcing (viz. SST and soil moisture anomaly) can be assumed to persist, the time averaged tropical circulation is highly predictable. In contrast, for the mid-latitudes, the day-to-day fluctuations are much larger, giving rise to a larger uncertainty in the estimates of time averages; and the effects of the changes in the boundary conditions at the earth's surface are relatively smaller.

In this paper we present results of actual forecast experiments for day-to-day weather changes as well as for space-time averaged circulation and show that the above conclusions which were based on predictability calculations are generally validated by actual forecast results.

A review of recent predictability and short-range prediction experiments for the tropics is presented in the next section. Following this, we have investigated the predictability of a moist model and compared it to that of a dry model in which diabatic heat sources are prescribed, thereby eliminating any interaction between the dynamics and the moist processes. It is found that the error growth rate for the dry model is only half as large as that for the moist model. This result is in agreement with the earlier results of Salstein (1976) and suggests that the interaction between dynamics and diabatic processes, as provided by the parametrisations of diabatic processes in current general circulation models, is a significant factor in determining the upper limit of theoretical predictability.

The section on 'Modelling of land surface processes' contains a brief summary of the results from medium-range forecast experiments with and without a simple biosphere model. We show that a better treatment of the biosphere (vegetation and soil characteristics) reduces systematic errors in ground temperature and surface heat fluxes and improves the prediction of diurnal changes of temperature and relative humidity at land points. In the following section we review some recent studies on the effects of SST anomalies on predictability of monthly and seasonal mean circulation and rainfall. It is found that the use of observed SST anomalies produces spectacular improvements in the prediction of monthly and seasonal average circulation and rainfall in the tropics. Finally we present a summary and concluding remarks.

Review of recent predictability and short-range prediction experiments for the tropics

These results can be described under the following three categories: (a) operational forecasts, (b) 'research' forecasts, and (c) 'perfect

model' forecasts (classical predictability experiments).

Operational forecasts

Figure 1 shows a time-series of the forecast day at which the 850 hPa total wind correlation for the tropics reaches 0.7 for the ECMWF (European Centre for Medium Range Weather Forecasting) operational forecast model. While it is encouraging to see that there has been a gradual improvement in the forecast skill since 1980, the current range of useful prediction for the tropics is found to be only 2-3 days.

Fig. 1 Forecast day on which the 850 hPa total wind correlation for the tropical belt, 18°S-18°N, reached 0.7.

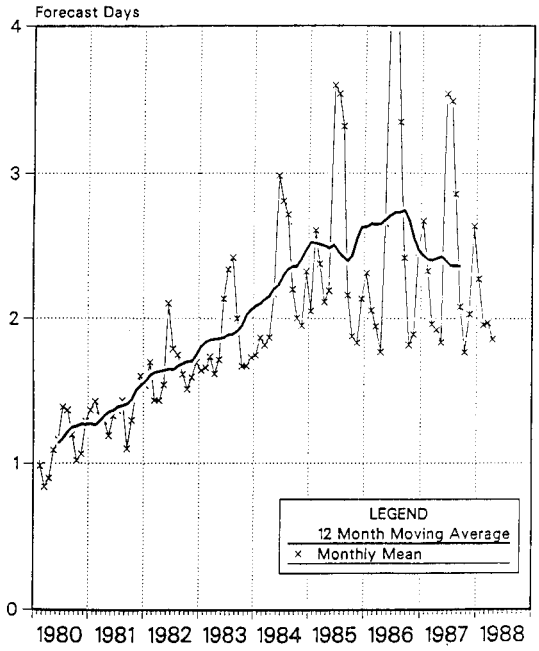

The performance of the ECMWF model for tropical forecasts has been reviewed earlier by Kanamitsu (1985) and Puri and Gauntlett (1987). It has been pointed out by Puri and Gauntlett (1987) that the ECMWF model produces significant systematic errors even in the short and medium-range forecasts. In a recent unpublished manuscript, Laurent et al. (1988)* have shown that the removal of systematic errors based on recent past forecasts improves the range of tropical predictability from 1-2 days to 3-5 days. Laurent et al. (1988), and Quah and Chang (1988)† have also shown that the propagation and development of westward moving disturbances over north Africa and South-East Asia respectively is predicted reasonably well up to 3-4 days. Generally, high amplitude waves are predicted better than weak amplitude disturbances. These results suggest that although the forecast skill defined in terms of the root mean square error over a large tropical area vanishes within 1-2 days, propagation, amplification and decay of well defined tropical wave disturbances can be predicted up to 3-4 days. Datta and Hatwar (1988) have evaluated the performance of the ECMWF model for short-range forecasting of summer monsoon rainfall over India. They conclude that although the seasonal average of the predicted rainfall at short-range compares well with the observed seasonal rainfall, short-range prediction of rainfall associated with individual monsoon depressions is not realistic.

'Research' forecasts

Results of research forecasts have been reported in numerous outstanding papers by Krishnamurti and his co-workers (see Krishnamurti 1988). By research forecasts, we mean prediction of a past event without the usual operational constraints and with the benefit of a more detailed analysis of observations to define the initial conditions. The number of such research forecasts is not sufficiently large to give statistical measures of forecast skill, but in some cases of research forecasts, displacements of individual disturbances can be predicted up to 5-6 days.

'Perfect model' forecasts

Figure 2 shows the results for forecasts of 200 hPa vector wind by the NMC (National Meteorological Center) model averaged for 30 cases of consecutive days starting from 14

* Laurent, H., Viltard, A. and De Felice, P. 1988. Performance evaluation and local adaptation of the 'ECMWF' system forecasts over north Africa for summer 1985. Available from ECMWF, Reading, UK.

† Quah, L. C. and Chang, B. K. 1988. Utilization of ECMWF global NWP products on GTS for operational weather forecasting at the Malaysian Meteorological Service (MMS). Paper presented at the WMO Technical Conference on Regional Weather Prediction with Emphasis on the Use of Global Products, 18-22 April 1988, ECMWF, Reading, UK. Available from the ECMWF, Reading, UK.

December 1986 (Tracton et al. 1988)*. Figure 2(a) is for the tropics (18°N-18°S) and Fig. 2(b) for the northern hemisphere mid-latitudes (22°N-70°N). The solid curve shows the forecast error, and the dashed curve shows the predictability error growth (i.e. the error growth for a perfect model) where initial error is equal to the one-day forecast error (see Lorenz 1982). It is found that the one-day tropical forecast error is already 50 per cent of the maximum possible forecast error and more than 70 per cent of the saturation value of the error. In contrast, for the mid-latitudes, the one-day forecast error is only 25 per cent of the maximum possible forecast error and less than 30 per cent of the saturation value of the error. The fact that the saturation value of the perfect model forecast error is significantly smaller than the maximum forecast error is indicative of a large systematic error in the tropics for this model.

We have also carried out similar calculations for the GFDL (Geophysical Fluid Dynamics Laboratory) model utilising an ensemble of 30-day forecasts reported by Miyakoda et al. (1986) in which they used eight different initial conditions. For each initial date, three different initial states obtained by three different analysis schemes (NMC, ECMWF and GFDL) were used for three separate integrations. We obtained a tape containing all the 30-day forecasts and observations for 500 hPa height used in this study and we calculated the predictability error growth and forecast errors for all of the eight initial conditions. The error growth was examined separately for the tropics and the mid-latitudes. Error between forecasts from different analyses is referred to as the perfect model forecast error in Fig. 3. It is quite clear that the saturation values of the forecast error for the tropics is far less than that for the mid-latitudes and the tropical error reaches its saturation value in only one day. It should be noted that most of the models, including the ECMWF model discussed above, showed similar results for 500 hPa heights. The above results for the NMC model and the GFDL model are in agreement with earlier results from the GLAS (Goddard Laboratory for Atmospheric Sciences) model (Shukla 1985).

* Tracton, S., Mo, K. C., Chen, W., Kalnay, E., Kistler, R. and White, G. 1988. Dynamical extended range forecasting (DERF) at National Meteorological Center. Available from National Meteorological Center, Washington D.C., USA.

Fig. 2 RMS forecast error (solid) and 'perfect model' forecast error (dashed) for 200 hPa vector wind for tropics (18°S-18°N), and mid-latitudes (22°N-70°N).

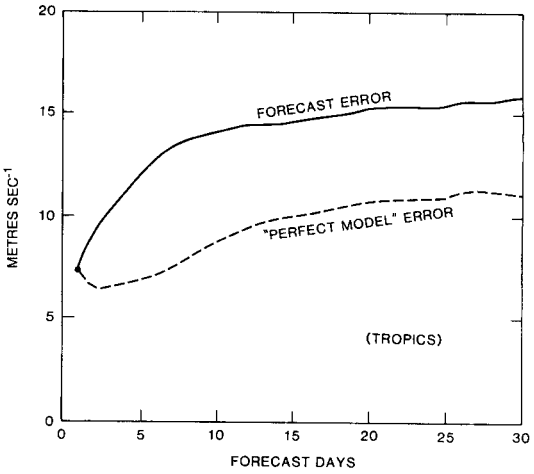

Fig. 3 RMS forecast error (solid) and 'perfect model' forecast error (dashed) for 500 hPa height for eight forecasts reported by Miyakoda et al. (1986) for mid-latitudes (22.5°S-70°N) and tropics (20°S-20°N).

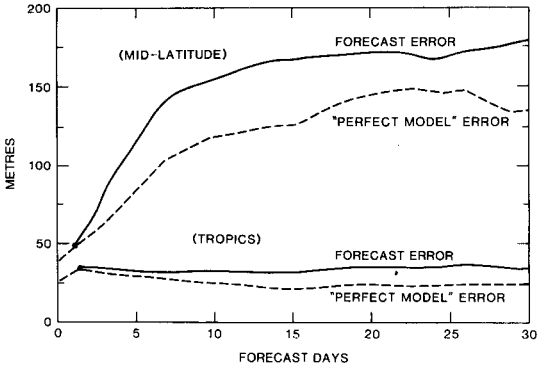

Predictability of dry and moist models

We have investigated the classical predictability of the NMC global spectral model (rhomboidal truncation, R40; 18 vertical layers; see Kinter et al. 1988) by first integrating the model for 10 days starting from the initial conditions of 15 and 25 December 1985, and then repeating the integrations with slightly perturbed initial conditions. The perturbations were introduced in all the prognostic variables of the model. Perturbations were obtained by subtracting two different model simulated states from a long model run and multiplying the difference by 0.1 to make the initial perturbation comparable to the uncertainties in the observations. The model was first integrated for 30 days (15 December 1985 through 14 January 1986) and the difference between model states on 4 January and 26 December was used to define one of the initial perturbations, to be referred to as P_1. All the calculations were repeated for another perturbation (P_2) which was defined by subtracting the model states on 14 January and 5 January. After scaling the initial perturbations, the globally averaged, root mean square (rms) difference for zonal wind at 500 hPa was found to be 1.1 m s^{-1} for P_1 and 0.68 m s^{-1} for P_2. The corresponding rms for temperature at 500 hPa was 0.4°C for P_1 and 0.26°C for P_2.

We have carried out four pairs of model integrations of the complete GCM (to be referred to as the moist model) to calculate the predictability error growth: two initial conditions (15 and 25 December 1985) and two perturbations (P_1 and P_2) on each of the two initial conditions.

We have repeated the above four pairs of integrations with a dry version of the complete general circulation model (GCM). The so-called dry model was constructed by eliminating all condensation processes (convective and large-scale supersaturation) from the model physics and replacing them by a prescribed heating obtained by averaging these fields from the one-month integration of the moist model described before. The radiative transfer calculations (which also depend upon the time varying temperature and moisture field) were replaced by a simple Newtonian cooling formulation in which zonally averaged model temperature is relaxed to a reference temperature which is obtained in such a way that a radiative relaxation time of 10 days will produce the same zonally averaged radiative heating and cooling as was produced by 30-day integration of the moist model. These modifications in the model physics make the moisture equation redundant in the dry model. It should be noted that these changes produce another source of temperature perturbation because the model uses virtual temperature rather than actual temperature; however, we found in a separate calculation that this effect was rather small.

We first used the dry model to carry out several 10-day forecasts starting from the observed initial conditions to examine its verisimilitude in predicting the observed day-to-day fluctuations. This is an important prerequisite for a model before it is used to study the factors responsible for the growth of initial errors in operational forecast models. Moreover, it would be appropriate to compare the predictability characteristics of the dry and moist models only if their ability to predict the evolution of the observed dynamical circulation is also comparable.

Figure 4 shows an example of a 10-day forecast starting from the observed initial conditions of 15 December 1986, both for the dry and the moist model. The three panels show the rms forecast error for zonal wind (U), meridional wind (V) and the zonally asymmetric geopotential height (Φ^*). For the geopotential height field we have verified only the departures from the zonal mean because the dry model showed a systematic forecast error in the zonally averaged height field. It can be seen from this figure that the global forecast rms error for all the variables is quite comparable. Therefore, it would be quite appropriate to compare the predictability characteristics of the two models.

Figures 5(a) and 5(b) give the predictability error growth averaged for both initial conditions for 200 hPa for perturbations P_1 and P_2 respectively. The four panels in each figure

Fig. 4 RMS forecast error for dry (dashed) and moist (solid) models for zonal wind (U), meridional wind (V) at 200 hPa and eddy geopotential (Φ^*) at 500 hPa.

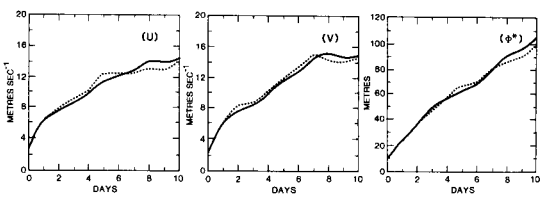

give results for zonal wind (U), meridional wind (V), geopotential (Φ) and temperature (T). It is seen that in each case the error growth rate for the moist model is higher than that for the dry model. The error growth for the moist model becomes significantly larger than that for the dry model after 4-5 days. It is likely that after 4-5 days the error is dominated by the synoptic scales, and if so, dynamics-moisture interaction is especially important for the predictability of synoptic scales and scales larger than the synoptic scales.

It was neither the purpose, nor would it be appropriate to conclude from these experiments that a dry model should be used for numerical weather prediction (NWP). The main point to be noted here is that although the dry model was a highly nonlinear dynamical system like the complete GCMs and the flow contained observed horizontal and vertical shears, thus allowing the growth of perturbations due to barotropic and baroclinic instabilities, the error growth was considerably reduced by simply removing the interaction between dynamics and moist processes. These results do suggest that some consideration should be given to the development of balanced models for which strong interaction between the high frequency changes in the flow and diabatic heating can be reduced for NWP.

Fig. 5(a) Error growth for dry (dashed) and moist (solid) models for zonal wind (U), meridional wind (V), geopotential height (Φ) and temperature (T) at 200 hPa. Initial perturbation (P_1).

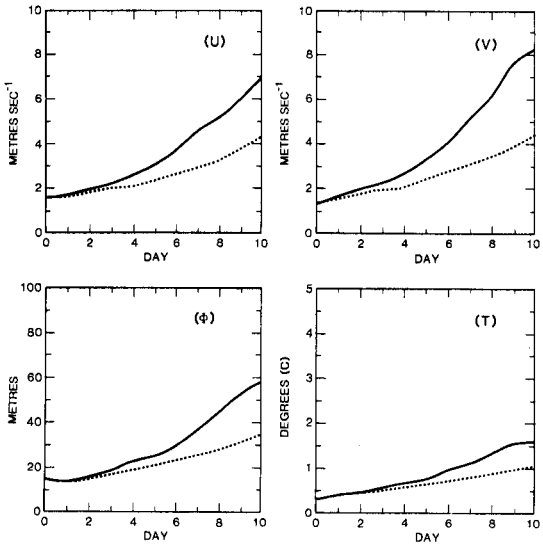

Fig. 5(b) Same as Fig. 5 (a) but for initial perturbation (P_2).

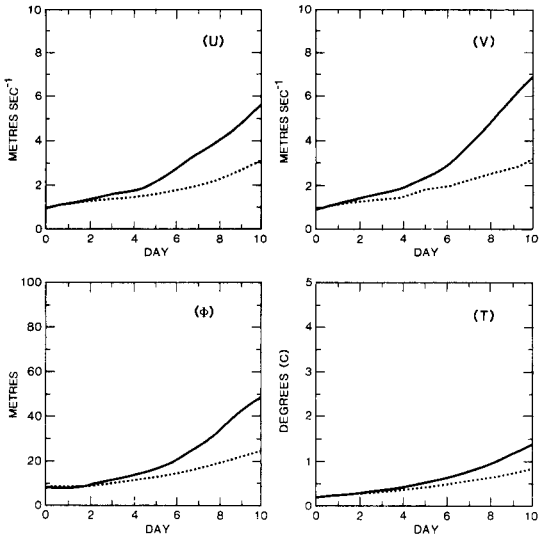

On the relative roles of radiative and condensation processes

For the experiments described in the earlier section, both the radiative as well as the condensation processes were simplified for the dry model. One additional experiment was carried out to investigate the relative effects of radiation and condensation. In this experiment, unlike the dry model case, the radiative heating was not simplified and the complete radiation code of the moist GCM was retained; only the condensation heating was specified like the dry model case. Thus, the only difference between this model and the dry model was that the dry model had the Newtonian cooling formulation for the radiative heating and this model had the complete radiation code of the GCM. A comparison of model integrations with the dry model and this model can provide some estimate of the effects of simplifying the radiation calculation alone. In one such comparison it was found that the effect of simplifying the radiation was rather small. It can be argued that this result could be a consequence of prescribed zonally symmetric cloudiness in the NMC model.

In a separate but related study we further investigated the role of radiation and condensation heating in generating eddy available potential energy. We integrated a global climate model (see Shukla et al. 1981) for one month starting from observed initial condi-

tions in winter and summer seasons. This model has diurnal variability and cloud-radiation interaction with model generated clouds that are variable in space and time.

Since generation of eddy available potential energy is one of the important internal processes which determines the dynamical evolution and energetics of the flow, the contribution of radiation and condensation in the short-term dynamical fluctuations can be measured by evaluating their contribution in generating eddy available potential energy. Figures 6(a) and 6(b) show the relative contributions of various diabatic processes and dynamical conversions in maintaining the balance of the eddy available potential energy. For the month of December (Fig. 6(a)), the globally and vertically averaged values of the generation of eddy available potential energy by long wave heating, short wave heating and non-radiative heating was found to be -0.04, 0.05 and 0.08 watts m^{-2}, whereas the conversions from the zonal potential energy to the eddy available potential energy, and from the eddy available potential energy to the eddy kinetic energy were 3.76 and 5.19 watts m^{-2} respectively. Likewise for a summer month (June, see Fig. 6(b)), the contributions of long wave, short wave and non-radiative heating were 0.05, 0.03 and 0.35 watts m^{-2} respectively, and the conversions from the zonal available potential energy to the eddy available potential energy, and the eddy available potential energy to the eddy kinetic energy were 2.92 and 4.17 watts m^{-2} respectively. It is seen that the dynamical conversion terms are far larger than the generation terms, and in particular, that the role of radiation in generating eddy available potential energy is quite small, especially because of cancellation of contributions from short wave and long wave.

We do not wish to present a detailed description and interpretation of these results in this paper. It may suffice to state that a detailed examination of the fields of radiative heating, condensation heating and temperature indicated that the field of condensation heating had large zonally asymmetric variability compared to the radiative heating field. The rainfall distribution which is a very good descriptor of the condensation heating field had pronounced local maxima giving rise to high spatial variance. In contrast, the radiative heating field did not have pronounced local maxima and minima and therefore less spatial variance. Since generation of eddy available potential energy is produced by correlation between the zonally asymmetric temperature and diabatic heating field, it is readily understandable as to why to the role of radiation was found to be insignificant.

Fig. 6(a) Vertical distribution of eddy available potential energy in units of watt pas cal^{-1} m^{-2} (abscissa) for the month of December, by short wave radiation (SW), long wave radiation (LW), non-radiative heating (NR), conversion from zonal to eddy available potential energy (CZE) and from eddy potential to eddy kinetic energy (CEK).

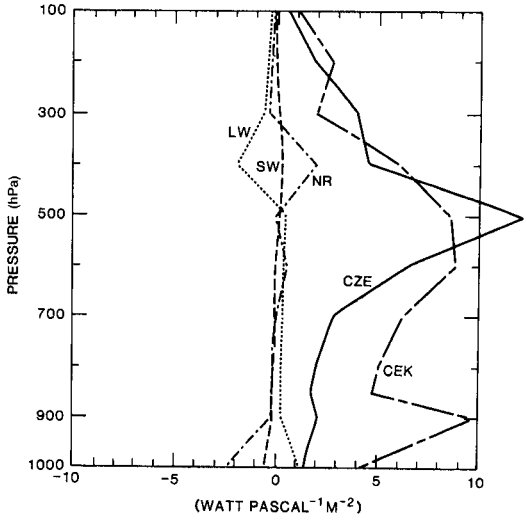

Fig. 6(b) Same as Fig. 6 (a) but for the month of June.

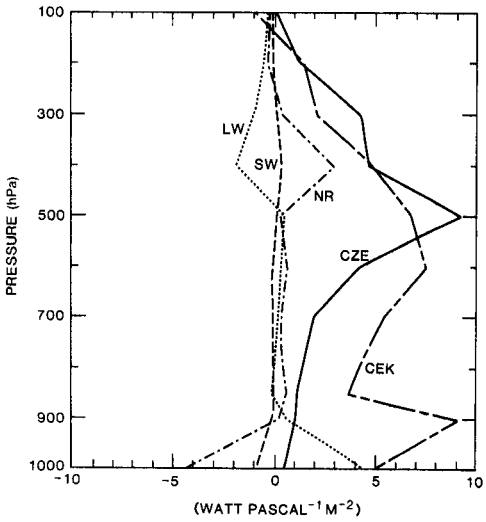

It should be noted, however, that these results are probably model-dependent and additional calculations with other GCMs and other cloud radiation schemes should also be carried out.

Modelling of land surface processes

As mentioned in the section 'Review of recent predictability and short-range prediction experiments for the tropics', one of the serious limitations of the current NWP models is the appearance of large systematic errors within a few days. This can be reduced only by gradual improvements in the model parametrisations. We present here some examples of medium-range forecasts with an improved treatment of the biosphere.

Traditionally, NWP and climate models prescribe, somewhat arbitrarily, the values of surface albedo, surface roughness and soil moisture at each of the land grid-points. It would be more appropriate to prescribe only the soil and vegetation characteristics, and albedo and roughness should be calculated in a physically consistent manner. This is the essence of some of the recent biosphere models (viz. Dickinson 1984; Sellers et al. 1986).

The biosphere model by Sellers et al. (1986) identifies each land grid-point with one of the twelve vegetation types and each vegetation type is defined by a set of morphological, physical and physiological parameters. The vegetation morphology is represented by bare soil, shrubs only, shrubs and ground cover, ground cover only, trees and ground cover, and trees only. There are three soil layers below ground: a thin upper layer, an intermediate layer (root zone), and a thick bottom layer (recharge zone). The model includes eight prognostic variables: canopy temperature, ground temperature, deep soil temperature, liquid water stored on canopy foliage and ground cover foliage, wetness of surface thin layer, root zone and recharge zone. The model uses atmospheric boundary conditions of wind speed, air temperature, incident radiative flux and precipitation. Run-off, soil moisture and sensible and latent heat flux are diagnostic outputs of the model.

Recently, Sato et al. (1989) have implemented this biosphere model in the NMC global spectral model described by Kinter et al. (1988). They found that the incorporation of the new biosphere model improved the diurnal cycle of temperature, sensible heat flux and evaporation. We have carried out 10-day forecasts with the NMC spectral model, with and without the biosphere model, for five different initial conditions in July 1986. The five initial conditions (July 1, 8, 15, 22 and 29) were arbitrarily chosen to be one week apart. Model forecasts without the biosphere model use the surface parametrisations described in Kinter et al. (1988) and will be referred to as the control model.

Figure 7 gives the difference of 10-day mean forecast 850 hPa temperature, with and without the biosphere model (biosphere minus control), averaged for all the five initial conditions. It is clearly seen that the biosphere model is warmer over the tropical land masses. Comparison of the control model forecasts with actual observations had shown that the control model tended to predict colder ground temperature over the land areas, and thus incorporation of the biosphere model somewhat reduced this deficiency of the model.

Fig. 7 Difference (biosphere model − control model) of 10-day mean forecast temperature (°C) at 850 hPa averaged for five different initial conditions in July 1986.

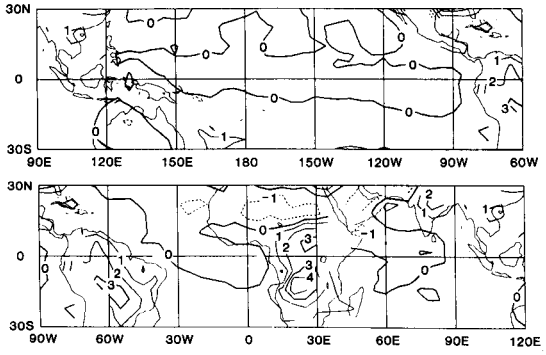

The most significant effect of the biosphere model is found to be in the prediction of the diurnal cycle of surface temperature and surface relative humidity. Figures 8(a) and 8(b) show the diurnal cycle of surface temperature for the control and biosphere model averaged for the five initial conditions for model grid-points near Washington, D.C. and Tallahas-

Fig. 8(a) Ensemble mean diurnal cycle of temperature (plotted for each time-step of 10 minutes) predicted by the biosphere model (dashed), the control model (solid) and hourly observations (solid line with dots) for a model grid-point near Washington, D.C.

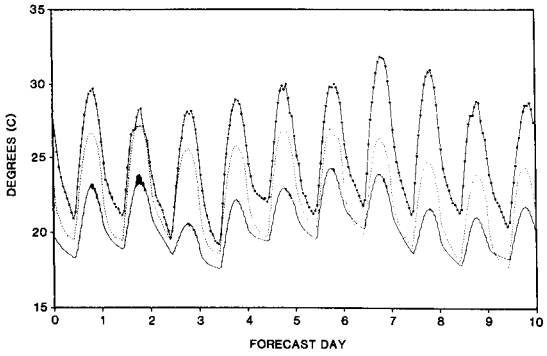

Fig. 8(b) Same as Fig. 8(a) but for a model grid-point near Tallahassee.

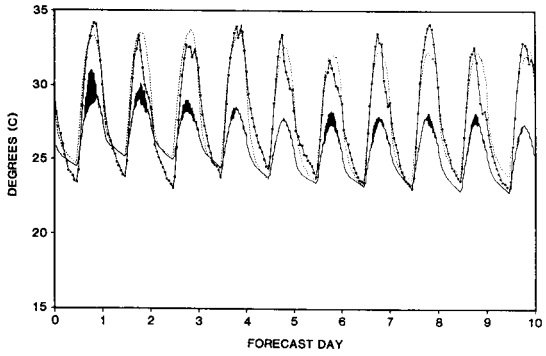

see, Florida, respectively. The model values were saved at each model time-step (12 minutes) and the observations for several stations within that model grid were obtained from NMC as hourly values. For the model grid-points labeled as Washington, D.C. and Tallahassee, there were 13 and 5 observation stations within those grid boxes, respectively. It is quite clear that the biosphere model produces a far more realistic diurnal cycle compared to the control model. The improvement in the prediction of the diurnal cycle of relative humidity by the biosphere model was even more spectacular. This was so mainly because the control model underpredicted the surface temperature and overpredicted the surface mixing ratio (because of too large evaporation and too small sensible heat flux) thereby predicting unrealistically large values of relative humidity.

It should be noted, however, that there was virtually no difference in the skill of the control and biosphere models for the prediction of hemispheric-scale height and circulation in the troposphere.

Predictability of space-time averages and the influence of the boundary conditions

There is a large body of modelling evidence which shows that prediction of 30 and 60-day average circulation and rainfall over the tropics is significantly improved if the observed, rather than the climatological, sea surface temperature (SST) is used for the lower boundary condition (WCRP 1986). Most of these numerical experiments have been carried out using the observed SST anomalies over the tropical and extratropical Pacific. Use of the observed SST correctly simulates the low-level moisture convergence and rainfall thereby producing more accurate descriptions of the tropical heat sources. Consequently, there is also some improvement in prediction of 30 and 60-day average circulation over the extratropics.

We present here some results from Shukla and Fennessy (1988) in which the GLAS model was integrated for 60 days starting from the observed initial conditions of 15, 16 and 17 December 1982 and using climatological seasonally varying SST boundary conditions. An ensemble average of these three integrations will be referred to as the control run. The above three integrations were repeated after modifying the Pacific SST (anomaly run). The observed SST anomaly for January 1983 which was used to modify the climatological SST is shown in Fig. 9. In the anomaly run SST is not modified over the region not shown in Fig. 9.

Fig. 9 Observed SST anomaly for January 1983.

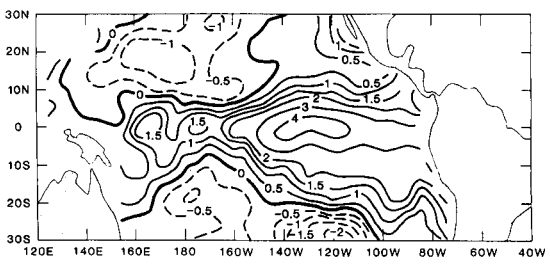

Figure 10 shows the observed rainfall anomaly for the same period. This is actually the observed anomaly of outgoing long wave radiation which has been converted into a rainfall anomaly using an empirical relation developed by Dr P. Arkin of the Climate Analysis Center. This is considered to be appropriate for model comparisons. Figure 10(b) shows the model simulated rainfall anomaly. This is the difference of the ensemble mean rainfall for the anomaly runs and the ensemble mean rainfall for the control runs for days 1-60. All the major centres of the rainfall anomaly are correctly predicted by the model.

Fig. 10 Simulated (top) and observed rainfall (bottom) anomaly (mm day^{-1}) for the winter season, 1983.

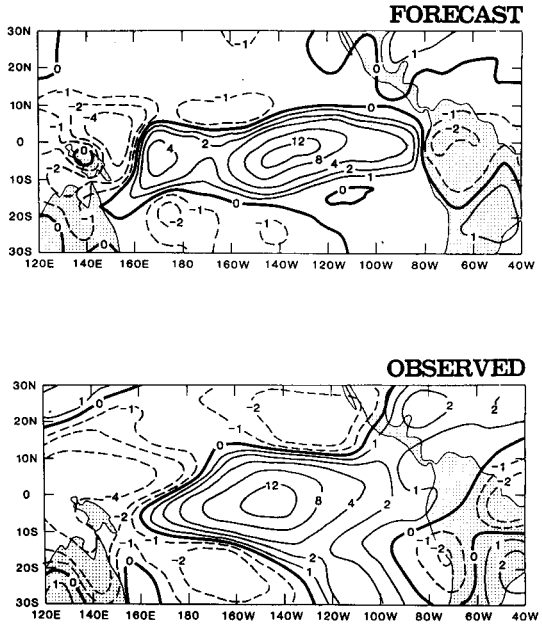

Figure 11 shows the forecast and observed geopotential anomaly at 300 hPa averaged for the periods 17 December 1982 to 16 February 1983. (A zonally averaged climate drift of the model calculated from several other independent integrations has also been removed from the model.) There is clear and unambiguous evidence that mid-latitude circulation anomalies are also affected by tropical heating anomalies.

Fig. 11 Simulated (top) and observed (bottom) 300 hPa height anomaly for the period 17 December 1982 to 16 February 1983.

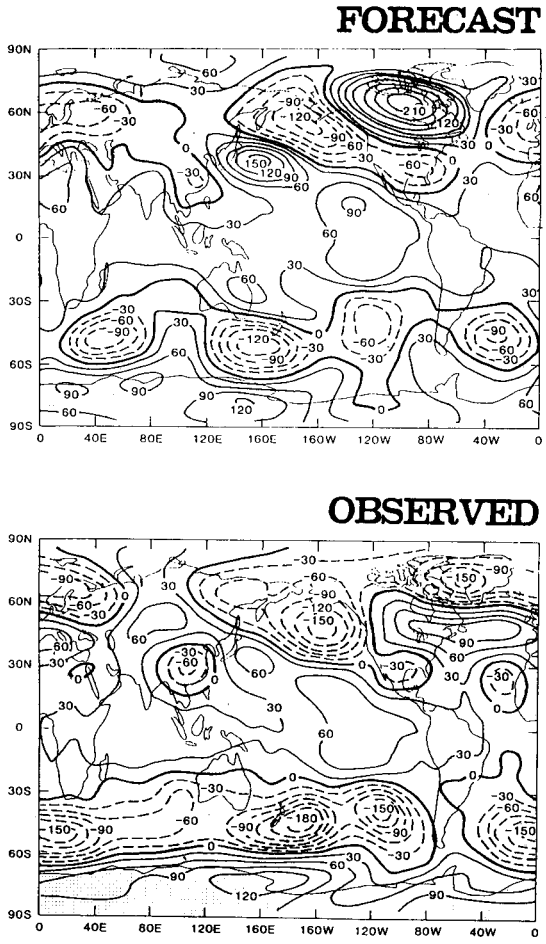

Figure 12(a) shows the time-series of 1000-200 hPa thickness for the region 30°N–30°S for control run, anomaly run and observations. There is a significant improvement in simulated thickness (and therefore temperature) using observed tropical SST anomalies. It should be noted that there are still significant errors, but perhaps some of those could be further reduced by taking into account other boundary conditions over the entire globe (SST, soil moisture, snow, sea ice, etc.).

Figure 12(b) shows the time-series of 200 hPa zonal wind averaged over a 10° latitude X 20° longitude equatorial box centred at 15°W and the equator for control runs and anomaly runs. The upper three thin curves

correspond to the three control runs starting from the initial conditions of 15, 16 and 17 December 1982. The thick curve is the ensemble average of the three control runs. Similarly, the middle three curves correspond to the anomaly runs using the same three initial conditions (15, 16 and 17 December 1982) and including the SST anomaly in the equatorial Pacific. The middle thick curve is the ensemble average of the three anomaly runs. The bottom starred curve is the observed zonal wind during the 1982-83 winter season averaged for the same box. All the curves represent 5-day running means of daily values.

It can be seen that the ensemble mean anomaly run values of zonal wind in the tropics are much closer to the observations than the control runs. Of course the anomaly runs still have large errors, but not as large as the control runs. Correct SST boundary conditions have corrected the tropical zonal wind forecasts quickly (within 10 days) and significantly.

Figure 13 shows the rms error for 300 hPa height for 10-day mean forecasts over the tropics (20°S–20°N) with and without SST anomaly and climate drift. It is clear that the inclusion of the SST anomaly makes a significant improvement in time mean forecasts.

Fig. 12(a) Time-series of 1000-200 hPa thickness for the tropical region (30°S-30°N) for model integrations with and without SST anomaly and observations.

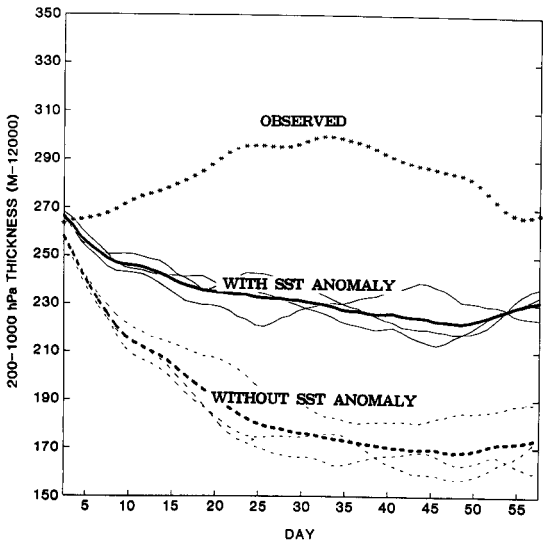

Fig. 12(b) Time-series of 200 hPa zonal wind for the equatorial Pacific (8°S-8°N, 157.5°W-137.5°W) for model integrations with and without SST anomaly and observations.

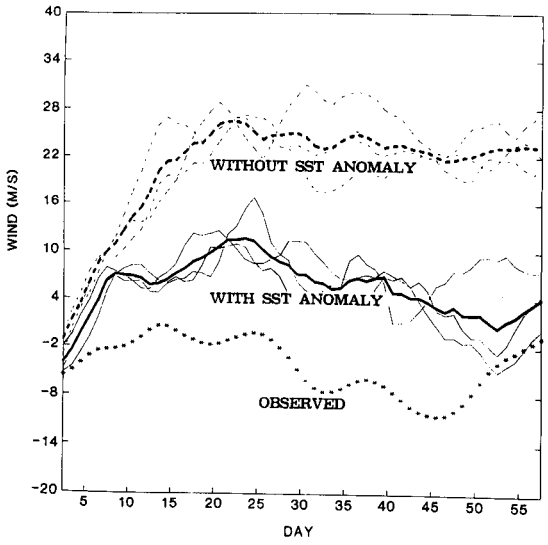

Fig. 13 RMS error for 10-day mean forecasts of 300 hPa height for the tropics (20°S-20°N) with and without SST anomaly and climate drift.

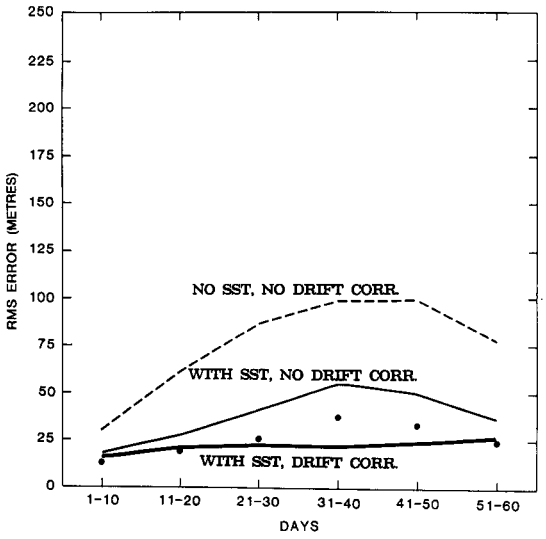

Likewise, the 300 hPa height anomaly correlation for 10-day forecasts for the region 58°S–58°N and 60°W–180°W, shown in Fig. 14, demonstrates the positive impact of the SST anomaly on extratropical forecasts.

Fig. 14 Anomaly correlation for 10-day mean forecasts of 300 hPa height with and without SST anomaly and climate drift for the region 58°S-58°N, 60°W-180°W.

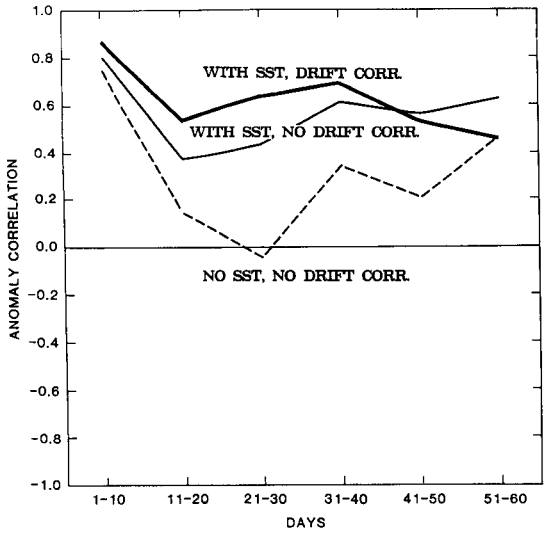

Summary and concluding remarks

We have examined both the forecast skill of current NWP models, and time-scales of predictability of the tropical atmosphere and concluded that, even if the errors in the initial conditions for NWP models and their growth rates were identical for the tropics and the mid-latitudes, the instantaneous flow patterns in the tropics would be far less predictable than those in the mid-latitudes. This is mainly so because the day-to-day variations in the tropics are much smaller and it takes only a few days for the initial error to grow to its saturation value. Partly for this reason and partly because the slowly varying boundary conditions at the earth's surface (SST, soil moisture, etc.) produce significant changes in the tropical circulation, the prospects for prediction of space-time averaged circulation and rainfall in the tropics are far higher than those for the mid-latitudes.

We have also carried out a few additional simple numerical experiments to address a more fundamental question of atmospheric predictability: What is the role of interaction between moist convection and atmospheric dynamics in determining the rate of growth of initial errors? Although we have not addressed this question separately for the tropics and the mid-latitudes, our preliminary calculations suggest that interactions between dynamics and condensation processes are an important and significant cause for the rapid growth of initial errors. Although this is not counterintuitive, it does suggest revision of the conventional notion that purely dynamical instabilities and nonlinearities can account for a rapid growth of small errors in the atmospheric models. In yet another set of numerical experiments we have shown that improvements in the treatment of vegetation and land-surface processes appear to produce significant improvements in prediction of the diurnal cycle.

Finally, we have summarised some of the earlier work on predictability of time averages which show that the use of observed sea surface temperature, in contrast to climatological sea surface temperature, produces spectacular improvements in the prediction of monthly and seasonal average circulation and rainfall in the tropics.

Acknowledgments

This paper is based on contributions from several scientists at COLA, ECMWF, NMC and GFDL. E. Albertazzi, Larry Marx and Mike Fennessy carried out most of the model calculations. Kiku Miyakoda and J. Sirutis provided the model forecasts and analyses and Brian Doty carried out the predictability calculations for the GFDL model. We would like to thank Tony Hollingsworth for providing information on the tropical forecast by ECMWF model and J.L. Kinter for reviewing the paper. Thanks to M. Schlichtig and S. Busching for the typing of this manuscript. This work was supported by NSF Grant ATM-87-13567 and by NASA Grants NAGW-557 and NAGW-558.

References

Charney, J.G. and Shukla, J. 1977. Predictability of monsoons. Symposium of Monsoon Dynamics, New Delhi, December 1977, published in *Monsoon Dynamics*, Cambridge University Press, Sir James Lighthill and R. P. Pearce (eds) (1981), 99-109.

Datta, R.K. and Hatwar, H.R. 1988. Prediction of monsoon rainfall over India with the ECMWF model. *Research Department Technical Memorandum No. 144*, ECMWF, Reading, UK, 20 pp.

Dickinson, R.E. 1984. Modeling evapotranspiration for three—dimensional global climate models. *Geophysical Monographs No. 19*, AGU, Washington D.C., USA, 58-72.

Kanamitsu, M. 1985. A study of predictability of the ECMWF operational forecast model in the tropics. *J. met. Soc. Japan, 63,* 779-804.

Kinter, J.L. III, Shukla, J., Marx, L. and Schneider, E.K. 1988. A simulation of the winter and summer circulations with the NMC global spectral model. *J. Atmos. Sci., 45,* 2486-522.

Krishnamurti, T.N. 1988. Some recent results on numerical weather prediction over the tropics. *Aust. Met. Mag., 36, 141-70.*

Lorenz, E.N. 1982. Atmospheric predictability experiments with a large numerical model. *Tellus, 34,* 505-13.

Miyakoda, K., Sirutis, J. and Ploshay, J. 1986. One-month forecast experiments—without boundary forcings. *Mon. Weath, Rev., 114,* 2363-401.

Puri, K. and Gauntlett, D.J. 1987. Numerical weather prediction in the tropics. *Short- and Medium-Range Numerical Weather Prediction,* Collection of Papers Presented at the WMO/IUGG NWP Symposium, Tokyo, Japan, 4-8 August 1986. T. Matsuno (ed), Meteorological Society of Japan, Tokyo, Japan, 605-31.

Salstein, D.A. 1976. Predictability of an atmosphere with large scale moisture patterns. PhD Thesis, M.I.T., Cambridge, MA, USA, 153 pp.

Sato, N., Sellers, P.J., Randall, D.A., Schneider, E.K., Shukla, J., Kinter, J.L. III, and Hou, Y.-T. 1989. Effects of implementing the simple biosphere model (SiB) in a general circulation model. *J. Almos. Sci., 46* (in press).

Sellers, P.J., Mintz, Y., Sud, Y.C. and Dalcher, A. 1986. A Simple Biosphere model (SiB) for use within general circulation models. *J. Atmos. Sci., 43,* 305-31.

Shukla, J. 1981. Predictability of the tropical atmosphere. *NASA Tech. Memo. 83829,* NASA Goddard Space Flight Center, Greenbelt, MD, USA, 51 pp.

Shukla, J. 1985. Predictability. Issues in atmospheric and oceanic modelling Part 11. Weather dynamics. *Adv. Geophys. Vol. 28B.* S. Manabe (ed.), Academic Press Inc., 87-122.

Shukla, J. and Fennessy, M.J. 1988. Prediction of time mean atmospheric circulation and rainfall: Influence of Pacific SST anomaly. *J. Atmos. Sci., 45,* 9-28.

Shukla, J., Straus, D.M., Randall, D., Sud, Y. and Marx, L. 1981. Winter and summer simulations with the GLAS climate model. *NASA Tech. Memo. 83866,* NASA Goddard Space Flight Center, Greenbelt, MD, USA, 282 pp.

World Climate Research Programme. 1986. Proceedings of the workshop on Comparison of Simulations by Numerical Models of the Sensitivity of the Atmospheric Circulation to Sea Surface Temperature Anomalies. *WMO/TD# 138, (WCP −121),* World Meteorological Organization, Geneva, 188 pp.